INSTITUT D'AERONOMIE SPATIALE DE BELGIQUE

3 - Avenue Circulaire
B - 1180 BRUXELLES

AERONOMICA ACTA

A - N° 169 - 1976

Field aligned distribution of plasma mantle and ionospheric plamas

by

J. LEMAIRE and M. SCHERER

BELGISCH INSTITUUT VOOR RUIMTE-AERONOMIE

3 - Ringlaan
B - 1180 BRUSSEL

FOREWORD

The article "Field aligned distribution of plasma mantle and ionospheric plasmas" was a contributed paper of "the Magnetopause Regions Symposium", hold at Amsterdam during the Third European Geophysical Society Meeting. It will be published in the Proceedings of the Symposium in one of the 1977 issues of the Journal of Atmospheric and Terrestrial Physics.

AVANT-PROPOS

L'article "Field aligned distribution of plasma mantle and ionospheric plasmas" est une contribution présentée au symposium intitulé "Proceedings of the Magnetopause Regions" et qui s'est tenu à Amsterdam du 7 au 10 septembre 1976 dans le cadre de la 3ème réunion de la European Geophysical Society. Ce texte sera publié dans les proceedings de symposium qui paraîtront dans un numéro spécial de Journal of Atmospheric and Terrestrial Physics.

VOORWOORD

De tekst "Field aligned distribution of plasma mantle and ionospheric plasmas" is een mededeling die gedaan werd tijdens de derde European Geophysical Society Meeting die plaats had te Amsterdam van 7 tot en met 10 september 1976. De tekst van deze mededeling zal gepubliceerd worden in de "Proceedings of the Magnetopause Regions Symposium" die zullen verschijnen in 1977 als een nummer van Journal of Atmospheric and Terrestrial Physics.

VORWORT

Der Tekst "Field aligned distribution of plasma mantle and ionospheric plasmas" ist ein Vortrag der in Amsterdam zum Symposium "Proceedings of the Magnetopause Regions" der während der dritten European Geophysical Society versammelung die September 7 - 10, 1976 gegeben worden ist. Dieses Artikel wird in die Proceedings dieses Symposium in ein Sonderausgang des Journal Atmospheric and Terrestrial Physics, veröffendlsicht.

FIELD ALIGNED DISTRIBUTION OF PLASMA MANTLE AND IONOSPHERIC PLASMAS

by

J. LEMAIRE and M. SCHERER

Abstract

The density and bulk velocity distributions of warm magnetosheath particles and cold ionospheric O^+ and H^+ ions are calculated along a polar cusp (cleft) magnetic field line. The warm collisionless plasma is injected at 12 Earth radii, and interacts with the cold polar wind electrons and ions of ionospheric origin. After magnetic reflections in the exosphere (above 1400 km altitude) most of the ions move upwards along tail magnetic field lines and feed the plasma mantle flow. The bulk velocity of these warm protons is approximately 200 km s^{-1} and happens to be proportional to the average thermal speed of the magnetosheath ions at their injection point in the magnetosphere. The density in the plasma mantle is found to be about two times smaller than in the entry layer. The electric potential distribution is deduced from the quasi-neutrality condition. A large parallel electric field corresponding to an electrostatic double layer is obtained for the assumed boundary conditions.

Résumé

Les distributions des densités et des vitesses moyennes de masse des particules de la magnetosheath et des ions O^+ et H^+ de l'ionosphère sont calculés le long d'une ligne de force magnétique pénétrant dans la Cusp (Cleft) polaire. Le plasma chaud est injecté à 12 rayons terrestres, et interagit avec les électrons et ions du vent polaire s'échappant de l'ionosphère supérieure. Après une réflexion magnétique dans l'exosphère (au-dessus de 1400 km d'altitude), la plupart des ions se meuvent vers l'extérieur le long des lignes de force de la queue géomagnétique et alimentent ainsi le "plasma mantle". La vitesse moyenne de masse de ces protons chauds est de l'ordre de 200 km/s. et s'avère être proportionnelle à la vitesse moyenne des ions de la magnetosheath, là où ceux-ci sont injectés dans la magnétosphère. La densité dans le "plasma mantle" est trouvée égale à la moitié de la densité dans la entry layer. Le potentiel électrique est déduit de la condition de quasi-neutralité. Un champ électrique très important est trouvé à 19000 km d'altitude où se situe dans le modèle considéré une double couche électrostatique.

Samenvatting

De dichtheid en stroomsnelheid van warme elektronen en protonen komende uit de magnetosheath, en koude zuurstof en waterstofionen evenals koude elektronen komende uit de ionosfeer wordt berekend langs een magnetische veldlijn in het Cusp (Cleft) gebied. Het warme plasma worden geinjecteerd op een afstand van 12 aardstralen. Na magnetische reflectie in de ionen-exosfeer stroomt het grootste deel van dit plasma langs een magnetische veldlijn in de staart van de magnetosfeer. De protonen stroomsnelheid bedraagt ongeveer 200 km s^{-1} en is evenredig met de gemiddelde thermische snelheid in het injectiegebied. De warme protonen hebben in de plasma mantel een dichtheid die ongeveer de helft is van hun dichtheid in het injectiegebied. De elektrische potentiaal die berekend wordt met behulp van de quasi-neutraliteitsvoorwaarde, geeft aanleiding tot een zeer sterk elektrisch veld dat het gevolg is van een elektrostatische dubbellaag.

Zusammenfassung

Die Dichte- und Geschmindigkeitsverteillungen der geladene Teilchen der Magnetosheath und die O^+ und H^+ Ionen der Ionosphäre sind entlangs Polar Cusp (Cleft) Feldlinien berechnet worden. Es ist an genommen dass das warme Magnetosheath-plasma won 11 Earth radii herunter injectiert ist and dass diese Teilchen mit den halten Ionen und Elektronen der Ionosphäre interagieren. Nach ein magnetische Reflexion in der Exosphäre (über 1400 km Höhe) bewegen sich meisten Ionen aüsserwertz und bilden de "Plasma Mantle" Fluss auf. Die mittelere Geschwindigkeit dieser warmen Protonen ist ungefähr 200 km/s und ist proportional mit der thermalen Geschwindigkeit der Magnetosheath Ionen who diese in der Magnetosphäre eindringen. Die Dichte im Plasma Mantle ist zwei Mal kleiner als die Dichte in der Entry Layer. Das elektrische Potential-verteillung ist von der Quasi-Neutralitäts Gleichung abgerechnet worden. Ein stränges parallel elektrisches Feld is in eine "Double Layer " in des Höhe 19000 km gefunden worden.

Six years ago, when we published our kinetic model for the polar ion-exosphere, we did not realize that the same kinetic approach would once apply rather well to describe the precipitation of Magnetosheath particles into the cusp, and that it could be used to model the tailward flow recently observed in the plasma mantle. In this short contributed paper we will not give a mathematical formulation of our standard kinetic model, but we will only discuss the numerical results obtained for one model calculation corresponding to reasonable boundary conditions at the exobase and entry layer. For those who are interested in a detailed description of the kinetic model we refer to some of our earlier papers (Lemaire and Scherer, 1971, 1972).

Figure 1 shows a meridional section of polar cusp flux tubes along which entry layer particles flow down on the equatorial side, and where plasma mantle particles flow up on the poleward side. Moreover, these flux tubes are filled from below with cold plasma of ionospheric origin. This cold plasma consists mainly of oxygen and hydrogen ions and cold electrons for which the densities and energies at the exobase level (1400 km) are summarized in Fig. 1. The number densities have been taken from ISIS II measurements (Hoffman *et al.*, 1974) at an altitude of 1400 km in the polar cusp which is very close to the level at which the Coulomb collisions between ionospheric particles become negligible. The energies at the exobase are conservative guesses corresponding to reasonable ionospheric temperatures. Finally, the flow velocities at the exobase are calculated from the first order moments of a truncated Maxwell-Boltzmann distribution which is empty in the downward loss cone.

The magnetosheath electrons and protons are assumed to be injected at high altitudes, with isotropic pitch angles except in the upward loss cone. At the exobase the densities of these warm particles have been choosen to obtain near the magnetopause a number density of 10 particles per cc for each kind and electron and proton temperatures of respectively 10^6 K and 7×10^6 K. Finally we also give in Fig. 1 the number densities and flow velocities in the entry layer at 69000 km, and in the plasma mantle at an altitude of 45000 km.

Six years ago, when we published our kinetic model for the polar ion-exosphere, we did not realize that the same kinetic approach would once apply rather well to describe the precipitation of Magnetosheath particles into the cusp, and that it could be used to model the tailward flow recently observed in the plasma mantle. In this short contributed paper we will not give a mathematical formulation of our standard kinetic model, but we will only discuss the numerical results obtained for one model calculation corresponding to reasonable boundary conditions at the exobase and entry layer. For those who are interested in a detailed description of the kinetic model we refer to some of our earlier papers (Lemaire and Scherer, 1971, 1972).

Figure 1 shows a meridional section of polar cusp flux tubes along which entry layer particles flow down on the equatorial side, and where plasma mantle particles flow up on the poleward side. Moreover, these flux tubes are filled from below with cold plasma of ionospheric origin. This cold plasma consists mainly of oxygen and hydrogen ions and cold electrons for which the densities and energies at the exobase level (1400 km) are summarized in Fig. 1. The number densities have been taken from ISIS II measurements (Hoffman *et al.*, 1974) at an altitude of 1400 km in the polar cusp which is very close to the level at which the Coulomb collisions between ionospheric particles become negligible. The energies at the exobase are conservative guesses corresponding to reasonable ionospheric temperatures. Finally, the flow velocities at the exobase are calculated from the first order moments of a truncated Maxwell-Boltzmann distribution which is empty in the downward loss cone.

The magnetosheath electrons and protons are assumed to be injected at high altitudes, with isotropic pitch angles except in the upward loss cone. At the exobase the densities of these warm particles have been choosen to obtain near the magnetopause a number density of 10 particles per cc for each kind and electron and proton temperatures of respectively 10^6 K and 7×10^6 K. Finally we also give in Fig. 1 the number densities and flow velocities in the entry layer at 69000 km, and in the plasma mantle at an altitude of 45000 km.

Six years ago, when we published our kinetic model for the polar ion-exosphere, we did not realize that the same kinetic approach would once apply rather well to describe the precipitation of Magnetosheath particles into the cusp, and that it could be used to model the tailward flow recently observed in the plasma mantle. In this short contributed paper we will not give a mathematical formulation of our standard kinetic model, but we will only discuss the numerical results obtained for one model calculation corresponding to reasonable boundary conditions at the exobase and entry layer. For those who are interested in a detailed description of the kinetic model we refer to some of our earlier papers (Lemaire and Scherer, 1971, 1972).

Figure 1 shows a meridional section of polar cusp flux tubes along which entry layer particles flow down on the equatorial side, and where plasma mantle particles flow up on the poleward side. Moreover, these flux tubes are filled from below with cold plasma of ionospheric origin. This cold plasma consists mainly of oxygen and hydrogen ions and cold electrons for which the densities and energies at the exobase level (1400 km) are summarized in Fig. 1. The number densities have been taken from ISIS II measurements (Hoffman *et al.*, 1974) at an altitude of 1400 km in the polar cusp which is very close to the level at which the Coulomb collisions between ionospheric particles become negligible. The energies at the exobase are conservative guesses corresponding to reasonable ionospheric temperatures. Finally, the flow velocities at the exobase are calculated from the first order moments of a truncated Maxwell-Boltzmann distribution which is empty in the downward loss cone.

The magnetosheath electrons and protons are assumed to be injected at high altitudes, with isotropic pitch angles except in the upward loss cone. At the exobase the densities of these warm particles have been choosen to obtain near the magnetopause a number density of 10 particles per cc for each kind and electron and proton temperatures of respectively 10^6 K and 7×10^6 K. Finally we also give in Fig. 1 the number densities and flow velocities in the entry layer at 69000 km, and in the plasma mantle at an altitude of 45000 km.

Above the exobase level the collisionless particles interact only through a charge separation electric field. This field can be derived from an electrostatic potential which must be a solution of Poisson's equation. Solving Poisson's equation along a magnetic field line is a very difficult problem which fortunately can be avoided whenever the electrostatic potential can be determined satisfactorily by imposing local charge neutrality at each altitude. Using this method we calculated the electric potential for the boundary conditions illustrated in Fig. 1, and for a potential difference of 25 Volts between the exobase and the magnetopause region. The results are plotted in Fig. 2. The shaded region below 1400 km is the collision-dominated region where the exospheric solutions are not valid. To extend the kinetic solution downwards into the lower ionosphere an hydrodynamic approach can be used (Lemaire, 1972; Lemaire and Scherer, 1975). As can be seen from Fig. 2 the electrostatic potential decreases monotonically from 25 Volts at the exobase, to almost zero at the magnetopause. At about 19000 km there exists a rather sharp potential drop or double-layer. At this altitude the corresponding parallel electric field, determined from the slope of the potential curve and shown in Fig. 3 has a peak intensity of 0.1 V/m (out of the frame of this figure). The thickness of this potential jump is approximately 50 meters which is about 2 times the local Debye length. Since in our one-dimensional model the double layer is perpendicular to the magnetic field, this result could be expected from the discussion of electrostatic shock waves by Kan (1975). For the more general case of an oblique double-layer the thickness will probably be of the order of a several ion gyroradii (Swift, 1975).

The density distributions of the different constituents are illustrated in Fig. 4. The number density of the oxygen ions, which is dominant at the exobase rapidly decreases with a scale height of 500 km. At 4500 km, the hydrogen ions become predominant, and finally at 13000 km the warm protons become the major ion species. Across the double-layer the ionospheric hydrogen density decreases sharply as a consequence of the impulsive acceleration of these escaping ions. This sudden acceleration is clearly illustrated in Fig. 5, where the flow velocity of the different kinds of particles are plotted : Once they have passed the double layer, the ionospheric hydrogen ions form a field aligned and almost mono-energetic stream moving upward with a flow speed of 70 km s^{-1}. The number density of the electrons of ionospheric origin has a very sharp decrease at the double-layer. This is due to the fact that almost all low energy electrons are reflected by the 25 Volt electrostatic potential

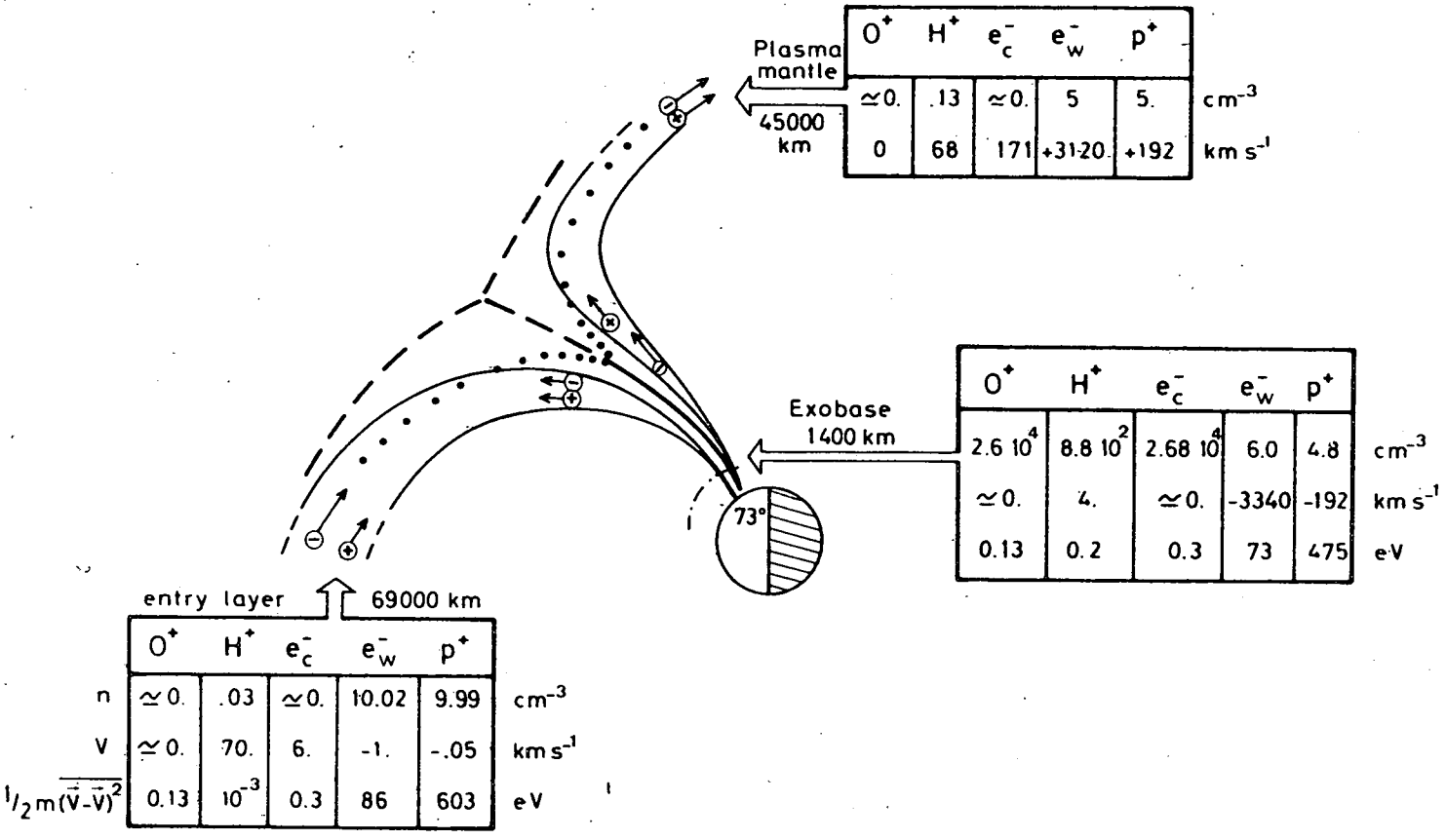

	O^+	H^+	e_c^-	e_w^-	p^+	
Plasma mantle, n	$\simeq 0.$	.13	$\simeq 0.$	5	5.	cm^{-3}
Plasma mantle, V	0	68	171	+31-20.	+192	$km\,s^{-1}$
Exobase, n	$2.6\,10^4$	$8.8\,10^2$	$2.68\,10^4$	6.0	4.8	cm^{-3}
Exobase, V	$\simeq 0.$	4.	$\simeq 0.$	-3340	-192	$km\,s^{-1}$
Exobase, $\frac{1}{2}m\overline{(\vec{V}-\vec{V})^2}$	0.13	0.2	0.3	73	475	eV
entry layer, n	$\simeq 0.$	.03	$\simeq 0.$	10.02	9.99	cm^{-3}
entry layer, V	$\simeq 0.$	70.	6.	-1.	-.05	$km\,s^{-1}$
entry layer, $\frac{1}{2}m\overline{(\vec{V}-\vec{V})^2}$	0.13	10^{-3}	0.3	86	603	eV

Fig. 1.- Meridional section of polar cusp flux tubes with assumed boundary conditions for the present model calculation.

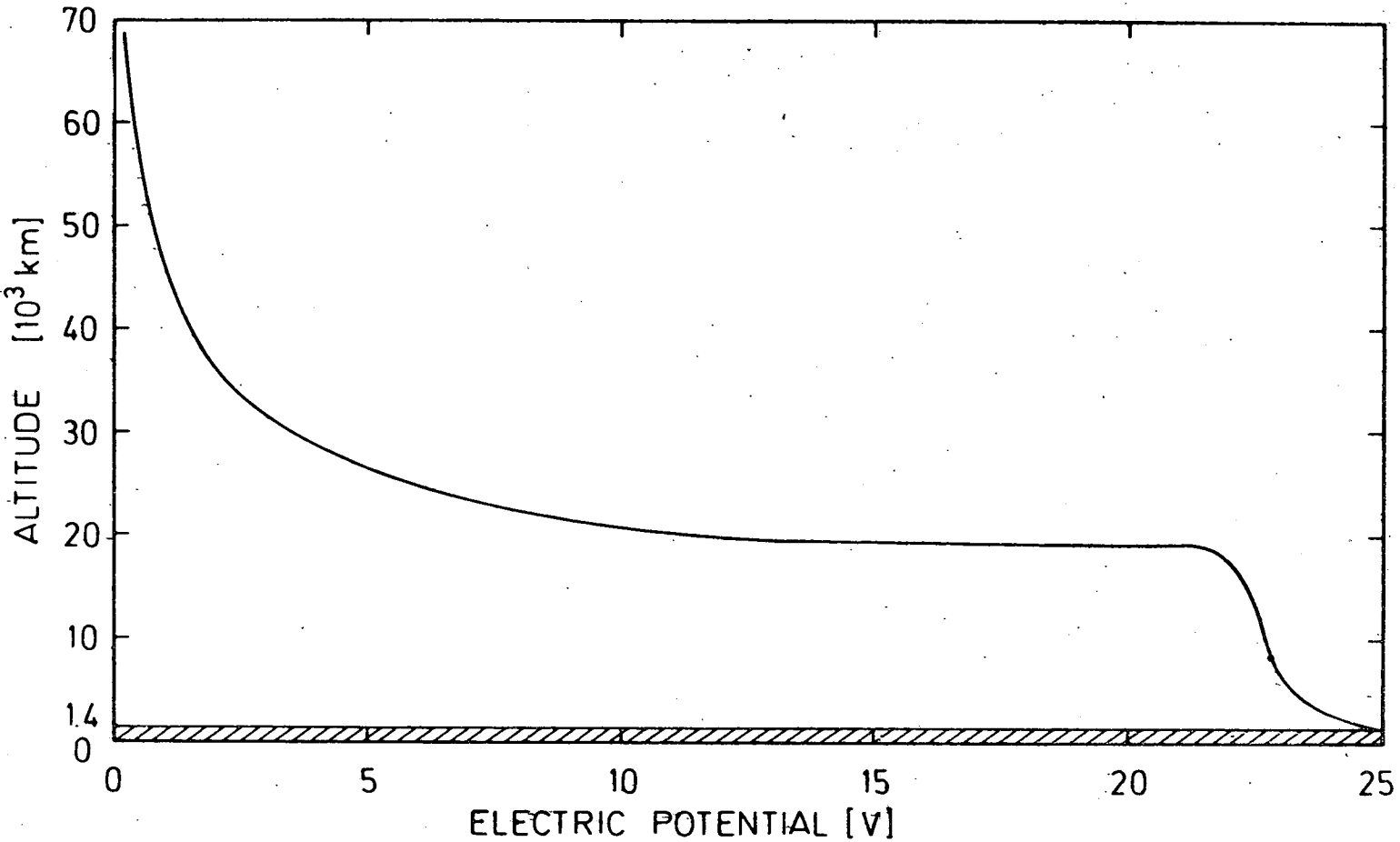

Fig. 2.- Electrostatic potential distribution in the collisionless region.

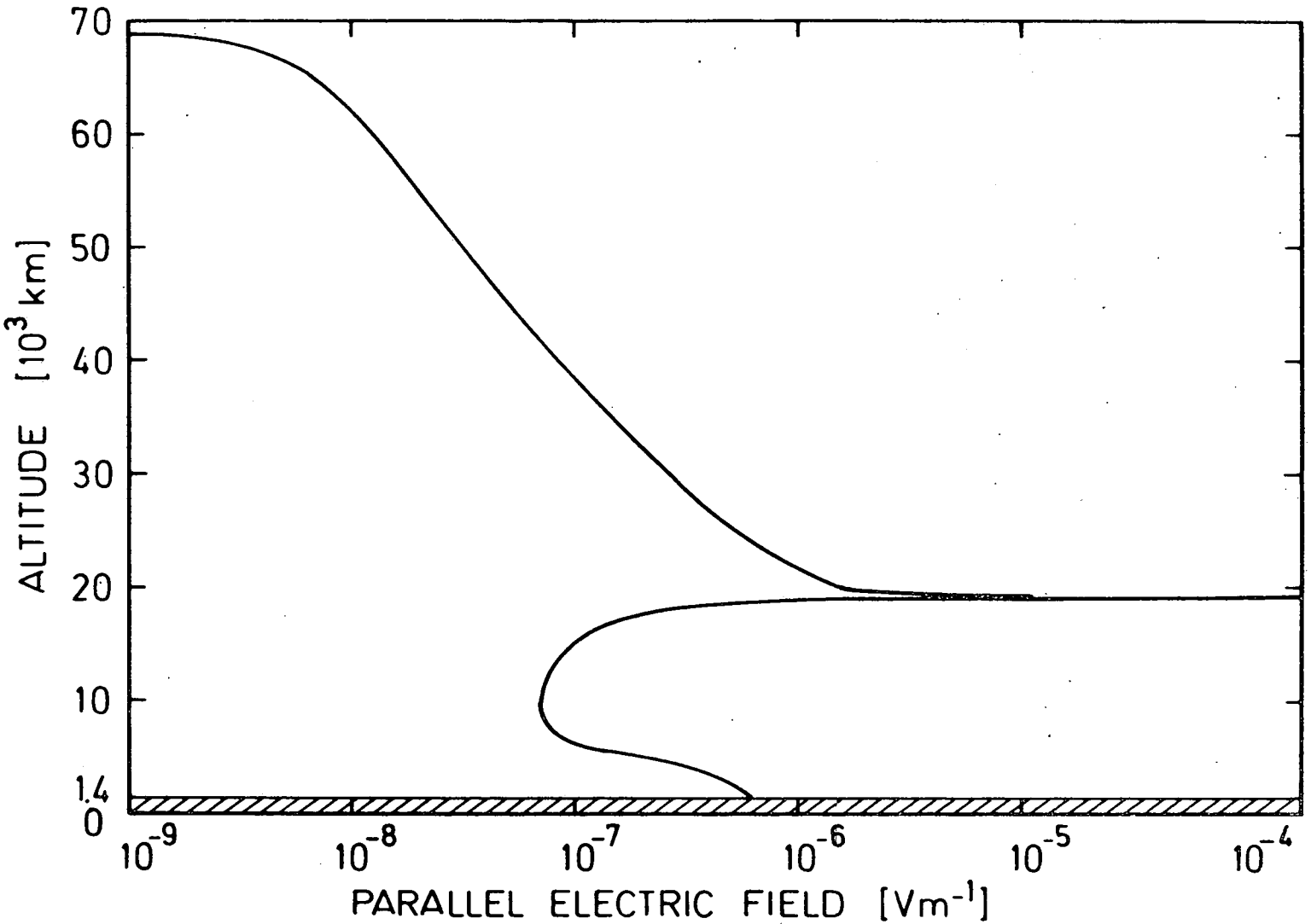

Fig. 3.- Parallel electric field distribution in the collisionfree region. The maximum value 0.1 Vm^{-1} reached at the double layer is out of the frame of this figure.

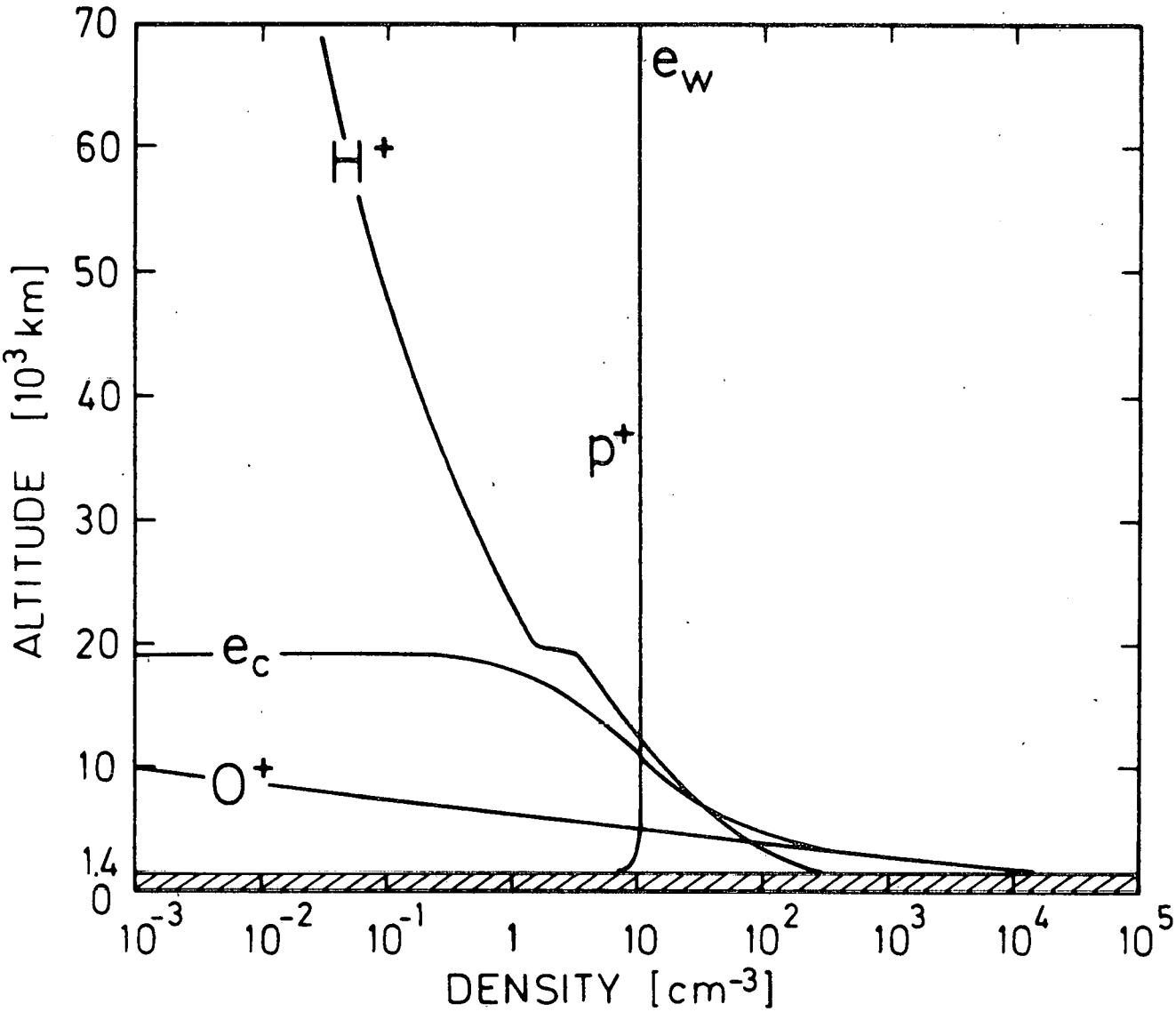

Fig. 4.- Number density distributions in the collisionfree region.

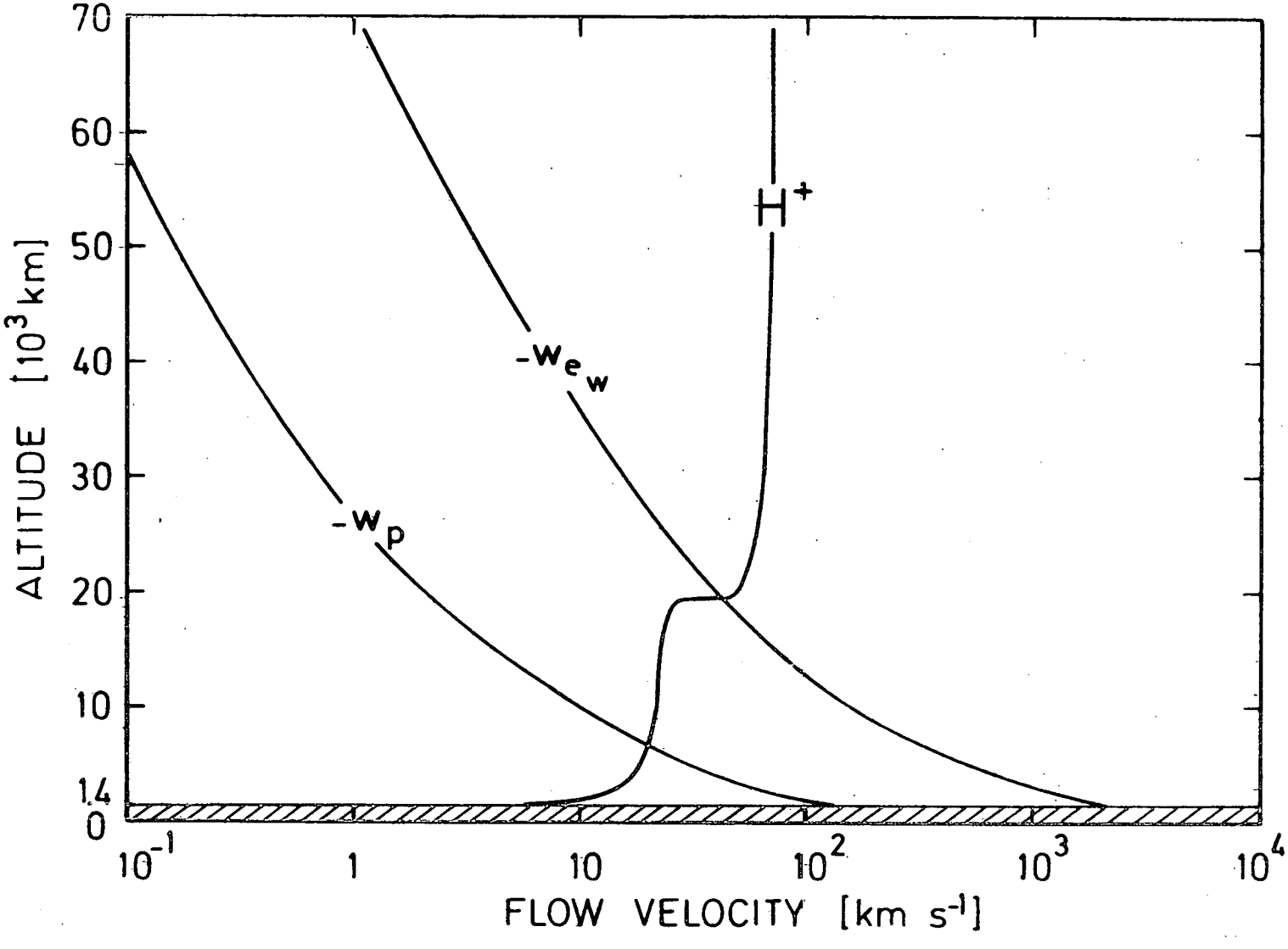

Fig. 5.- Flow velocities in the collisionfree region, calculated under the assumption that particles reflected above the exobase do not contribute to the net flux.

barrier, and therefore the cold electrons form a cushion of trapped particles on which the double layer rests. The escape flux of these ionospheric electrons is also very small as a consequence of the high potential barrier and the flow velocity near the exobase is almost zero.

The flow velocity of the hot protons is directed downwards in the entry layer and is only $50\ ms^{-1}$ at the equator. This low velocity results from the small fraction of precipitating particles compared to those who are injected with a pitch angle outside the narrow loss cone. However, when the altitude decreases the loss cone opens and the flow velocity of the warm particles increases proportionally to the magnetic field intensity. At the top of the ionosphere the precipitating protons have reached a downward flow speed of $200\ km\ s^{-1}$. This apparent acceleration is only a consequence of the convergence of the magnetic field lines. Magnetosheath alpha particles which are injected with a temperature 4 times larger than the warm proton temperature will have nearly the same flow velocity as the protons (cfr. Table 1). These calculated alpha and proton flow velocities are consistent with recent observations made at 800 km by Shelley *et al.* (1976) and are also supported by the observations in the entry layer (Paschmann *et al.*, 1976).

The number density of the hot protons and electrons are plotted in Fig. 4. They do not vary much with altitude and they are almost equal. However, plotting these densities with a linear density scale shows that there exists a difference between both kinds of particles. This is clearly illustrated in Fig. 6 : at altitudes lower than the electrostatic double layer the number density of the warm electrons exceeds the warm proton number density by 2-3 particles per cc. Above the double layer this difference is much smaller and tends to negligibly small values at high altitudes.

The flow velocity of the hot electrons has a similar behavior as the flow speed of the magnetosheath protons but is much larger in absolute value. These precipitating electrons of magnetosheath origin carry the largest fraction of the field aligned electric current. This is illustrated in table 1, where the different fractional parallel currents corresponding to each kind of particles are give at the exobase level. The results summarized in this table were

Table 1.- The fractional mass fluxes (4th column) and parallel electric current densities (last column) for each kind of particles (1 st column) at the exobase level (1400 km). The densities (2nd column) and temperatures (3th column) are also given. The potential difference between the exobase and the magnetopause region is assumed to be 25 Volts.

j	$n[cm^{-3}]$	T[K]	$m\ n\ w\ [kg\ m^{-2}\ s^{-1}]$	$J_{\parallel}[A\ m^{-2}]$
e_c	26914.	3500	0	0
O^+	26000.	1500	0	0
H^+	880.	3000	5.8×10^{-15}	5.6×10^{-7}
He^+	34.	3000	4.5×10^{-16}	1.1×10^{-8}
e_w	6.5	10^6	-2.0×10^{-17}	3.5×10^{-6}
p^+	4.8	7×10^6	-1.5×10^{-15}	-1.5×10^{-7}
He^{++}	0.2	3×10^7	-2.6×10^{-16}	-1.3×10^{-8}
TOTAL	0	-	4.5×10^{-15}	3.9×10^{-6}

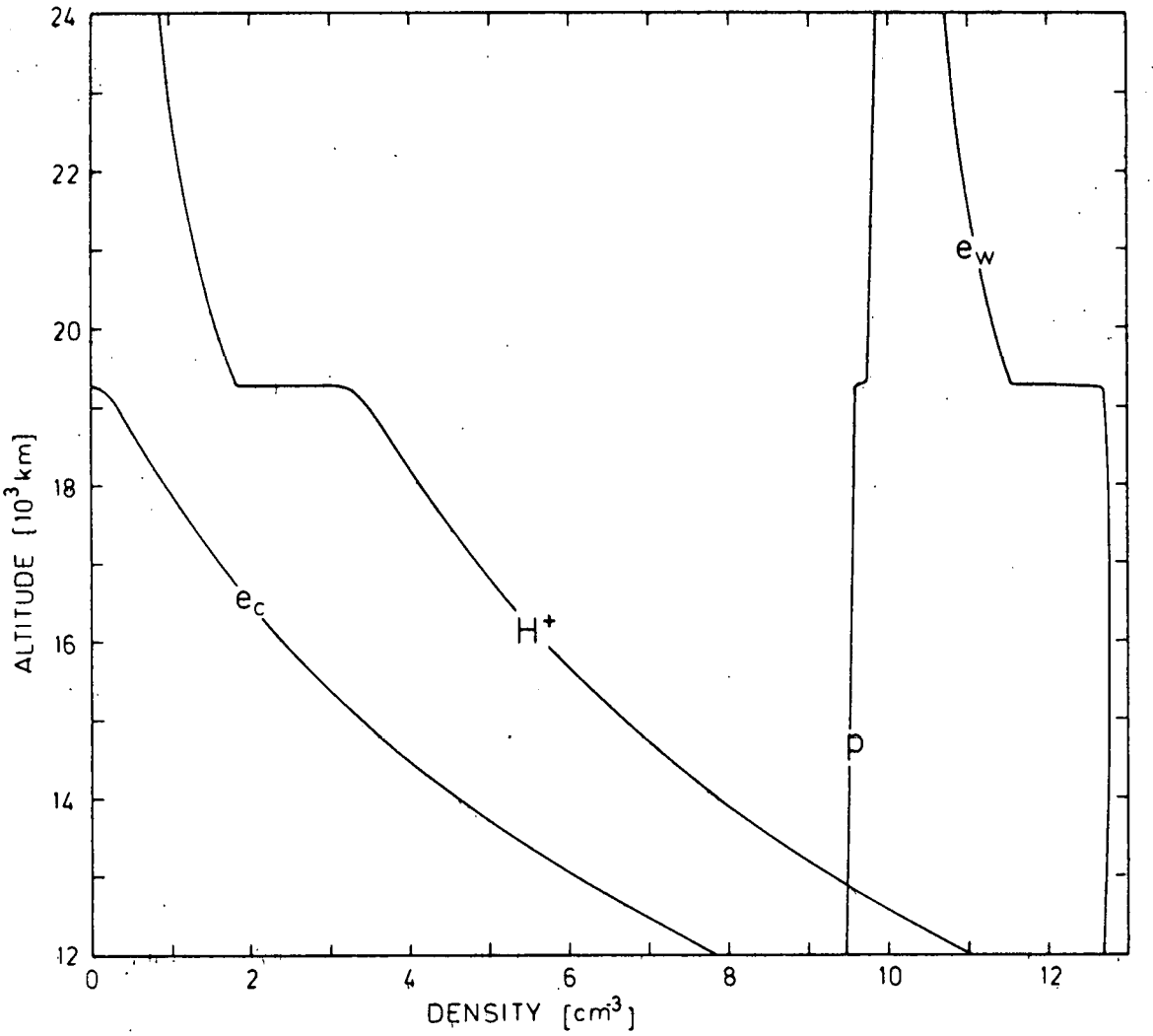

Fig. 6.- Number density distribution in a part of the collisionfree region.

obtained for similar boundary conditions as above but with the additional presence of a small quantity of ionospheric helium ions and precipitating α-particles. The values of the parallel current densities are given in the last column : positive values correspond to upward currents, negative values to downward currents. The warm magnetosheath electrons transport 90% of the total upward directed electric current. The largest mass flux, however is carried by the escaping ionospheric hydrogen ions (see table 1, column 3).

Finally, in Fig. 7 we plotted again the (downward directed) flow velocities of the warm protons and electrons calculated under the assumption that particles reflected above the exobase do not contribute to the net flux in the entry layer. However, assuming with Rosenbauer *et al.* (1975) that the plasma mantle is composed of magnetosheath particles which have been mirrored and have drifted polewards in the midaltitude cusp region, we estimated the upward flow speed in the plasma mantle. This calculation showed that the tailward flow velocity (u_p in Fig. 7) of the magnetosheath protons is 200 km s^{-1} which is approximately half the thermal speed at the injection point in the magnetosphere. Therefore, according to this model calculation it can be suggested that the ion flow velocity in the plasma mantle is proportional to the square root of the dayside magnetosheath proton temperature.

According to the present kinetic calculation the density in the plasma mantle is half that in the entry layer. The calculated density and flow velocity of the warm protons in the plasma mantle and entry layer seem to be in agreement with the observations (Paschmann and Haerendel, 1976; Sckopke and Paschmann, 1976).

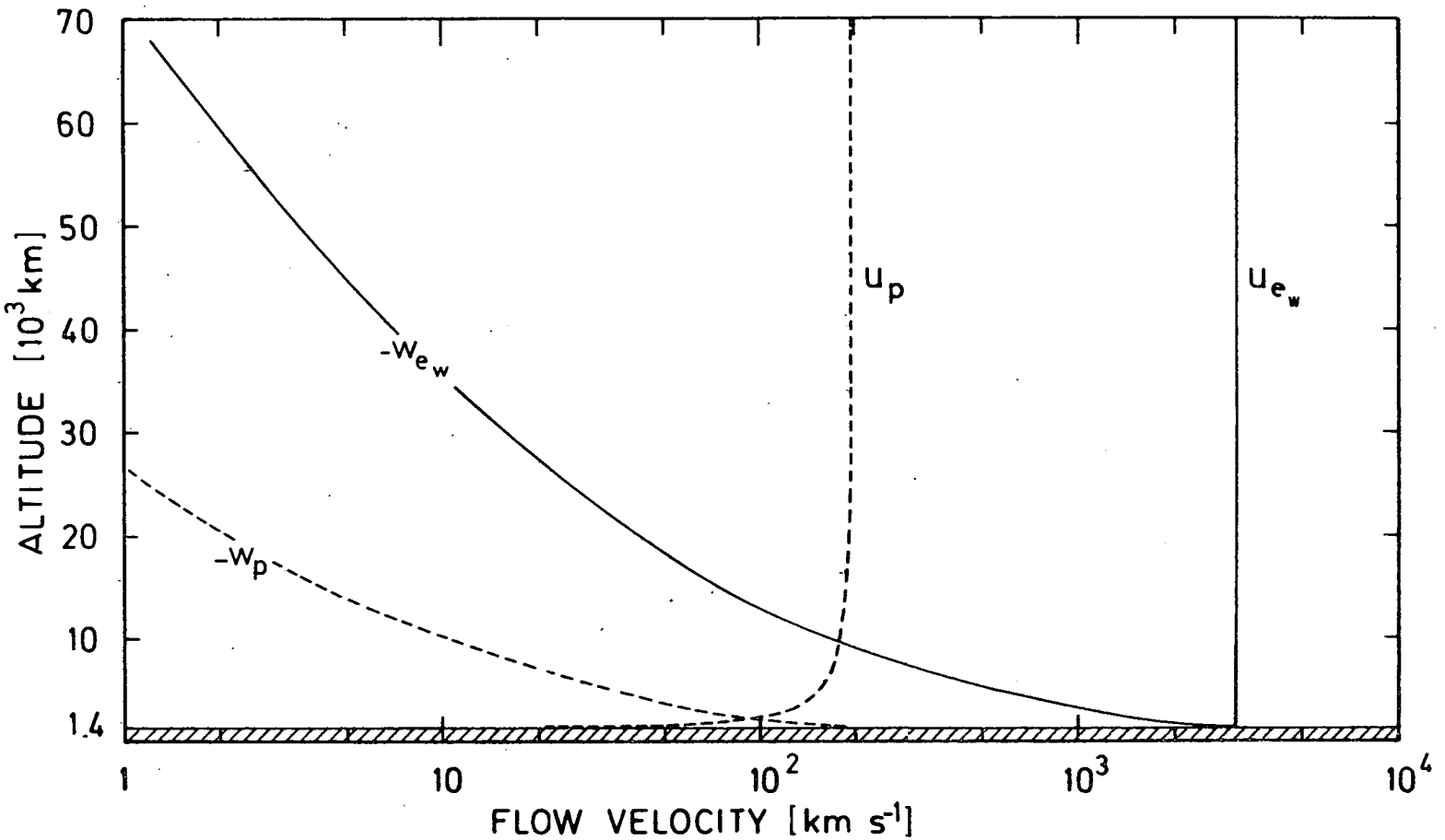

Fig. 7.- Flow velocities in the collisionfree region : u_p and u_{e_w} are calculated under the assumption that the downward flux of the warm particles is zero in the plasma mantle.

REFERENCES

HOFFMAN J.H., W.H. DODSON, C.R. LIPPINCOTT, and H.D. HAMMACK, *J. Geophys. Res.*, **79**, 4246, 1974.

KAN J.R., *J. Geophys. Res.*, **80**, 2089, 1975.

LEMAIRE J., *J. Atmos. Terr. Phys.*, **34**, 1647, 1972.

LEMAIRE J. and M. SCHERER, *Phys. Fluids*, **14**, 1683, 1971.

LEMAIRE J. and M. SCHERER, *Phys. Fluids*, **15**, 760, 1972.

LEMAIRE J. and M. SCHERER, *Aeronomica Acta A*, **147**, 1975.

PASCHMANN G. and G. HAERENDEL, *Trans. Am. Geophys. Union*, **57**, 662 1976 .

PASCHMANN G., G. HAERENDEL, N. SCHKOPKE, H. ROSENBAUER and P.C. HEDGECOCK, *J. Geophys. Res.*, **81**, 2883, 1976.

ROSENBAUER H., H. GRUNWALDT, M.D. MONTGOMERY, G. PASCHMANN and N. SCHKOPKE, *J. Geophys. Res.*, **80**, 2723, 1975.

SCHKOPKE N. and G. PASCHMANN, *Trans. Am. Geophys. Union*, **57**, 662 1976 .

SHELLEY E.G., D. SHARP and R.G. JOHNSON, *J. Geophys. Res.*, **81**, 2363, 1976.

SWIFT D.W., *J. Geophys. Res.*, **80**, 2096, 1975.

100 - BIAUME, F., Détermination de la valeur absolue de l'absorption dans les bandes du système de Schumann-Runge de l'oxygène moléculaire, 1972.

101 - NICOLET, M. and W. PEETERMANS, The production of nitric oxide in the stratosphere by oxidations of nitrous oxide, 1972.

102 - VAN HEMELRIJCK, E. et H. DEBEHOGNE, Observations au Portugal de phénomènes lumineux se rapportant a une expérience de lâcher de barium dans la magnétosphère, 1972.

103 - NICOLET, M. et W. PEETERMANS, On the vertical distribution of carbon monoxide and methane in the stratosphere, 1972.

104 - KOCKARTS, G., Heat balance and thermal conduction, 1972.

105 - ACKERMAN, M. and C. MULLER, Stratospheric methane from infrared spectra, 1972.

106 - ACKERMAN, M. and C. MULLER, Stratospheric nitrogen dioxide from infrared absorption spectra, 1972.

107 - KOCKARTS, G., Absorption par l'oxygène moléculaire dans les bandes de Schumann-Runge, 1972.

108 - LEMAIRE, J. et M. SCHERER, Comportements asymptotiques d'un modèle cinétique du vent solaire, 1972.

109 - LEMAIRE, J. and M. SCHERER, Plasma sheet particle precipitation : A kinetic model, 1972.

110 - BRASSEUR, G. and S. CIESLIK, On the behavior of nitrogen oxides in the stratosphere, 1972.

111 - ACKERMAN, M. and P. SIMON, Rocket measurement of solar fluxes at 1216 Å, 1450 Å and 1710 Å, 1972.

112 - CIESLIK, S. and M. NICOLET, The aeronomic dissociation of nitric oxide, 1973.

113 - BRASSEUR, G. and M. NICOLET, Chemospheric processes of nitric oxide in the mesosphere and stratosphere, 1973.

114 - CIESLIK, S. et C. MULLER, Absorption raie par raie dans la bande fondamentale infrarouge du monoxyde d'azote, 1973.

115 - LEMAIRE, J. and M. SCHERER, Kinetic models of the solar and polar winds, 1973.

116 - NICOLET, M., La biosphère au service de l'atmosphère, 1973.

117 - BIAUME, F., Nitric acid vapor absorption cross section spectrum and its photodissociation in the stratosphere, 1973.

118 - BRASSEUR, G., Chemical kinetic in the stratosphere, 1973.

119 - KOCKARTS, G., Helium in the terrestrial atmosphere, 1973.

120 - ACKERMAN, M., J.C. FONTANELLA, D. FRIMOUT, A. GIRARD, L. GRAMONT, N. LOUISNARD, C. MULLER and D. NEVEJANS, Recent stratospheric spectra of NO and NO_2, 1973.

121 - NICOLET, M., An overview of aeronomic processes in the stratosphere and mesosphere, 1973.

122 - LEMAIRE, J., The "Roche-Limit" of ionospheric plasma and the formation of the plasmapause, 1973.

123 - SIMON, P., Balloon measurements of solar fluxes between 1960 Å and 2300 Å, 1974.

124 - ARIJS, E., Effusion of ions through small holes, 1974.

125 - NICOLET, M., Aëronomie, 1974.

126 - SIMON, P., Observation de l'absorption du rayonnement ultraviolet solaire par ballons stratosphériques, 1974.

127 - VERCHEVAL, J., Contribution à l'étude de l'atmosphère terrestre supérieure à partir de l'analyse orbitale des satellites, 1973.

128 - LEMAIRE, J. and M. SCHERER, Exospheric models of the topside ionosphere, 1974.

129 - ACKERMAN, M., Stratospheric water vapor from high resolution infrared spectra, 1974.

130 - ROTH, M., Generalized invariant for a charged particle interacting with a linearly polarized hydromagnetic plane wave, 1974.

131 - BOLIN, R.C., D. FRIMOUT and C.F. LILLIE, Absolute flux measurements in the rocket ultraviolet, 1974.

132 - MAIGNAN, M. et C. MULLER, Méthodes de calcul de spectres stratosphériques d'absorption infrarouge, 1974.

133 - ACKERMAN, M., J.C. FONTANELLA, D. FRIMOUT, A. GIRARD, N. LOUISNARD and C. MULLER, Simultaneous measurements of NO and NO_2 in the stratosphere, 1974.

134 - NICOLET, M., On the production of nitric oxide by cosmic rays in the mesosphere and stratosphere, 1974.

135 - LEMAIRE, J. and M. SCHERER, Ionosphere-plasmasheet field aligned currents and parallel electric fields, 1974.

136 - ACKERMAN, M., P. SIMON, U. von ZAHN and U. LAUX, Simultaneous upper air composition measurements by means of UV monochromator and mass spectrometer, 1974.

137 - KOCKARTS, G., Neutral atmosphere modeling, 1974.

138 - BARLIER, F., P. BAUER, C. JAECK, G. THUILLIER and G. KOCKARTS, North-South asymmetries in the thermosphere during the last maximum of the solar cycle, 1974.

139 - ROTH, M., The effects of field aligned ionization models on the electron densities and total flux tubes contents deduced by the method of whistler analysis, 1974.

140 - DA MATA, L., La transition de l'homosphère à l'hétérosphère de l'atmosphère terrestre, 1974.

141 - LEMAIRE, J. and R.J. HOCH, Stable auroral red arcs and their importance for the physics of the plasmapause region, 1975.

142 - ACKERMAN, M., NO, NO_2 and HNO_3 below 35 km in the atmosphere, 1975.

143 - LEMAIRE, J., The mechanisms of formation of the plasmapause, 1975.

144 - SCIALOM, G., C. TAIEB and G. KOCKARTS, Daytime valley in the F1 region observed by incoherent scatter, 1975.

145 - SIMON, P., Nouvelles mesures de l'ultraviolet solaire dans la stratosphère, 1975.

146 - BRASSEUR, G. et M. BERTIN, Un modèle bi-dimensionnel de la stratosphère, 1975.

147 - LEMAIRE, J. et M. SCHERER, Contribution à l'étude des ions dans l'ionosphère polaire, 1975.

148 - DEBEHOGNE, H. et E. VAN HEMELRIJCK, Etude par étoiles-tests de la réduction des clichés pris au moyen de la caméra de triangulation IAS, 1975.

149 - DEBEHOGNE, H. et E. VAN HEMELRIJCK, Méthode des moindres carrés appliquée à la réduction des clichés astrométriques, 1975.

150 - DEBEHOGNE, H. et E. VAN HEMELRIJCK, Contribution au problème de l'abérration différentielle, 1975.

151 - MULLER, C. and A.J. SAUVAL, The CO fundamental bands in the solar spectrum, 1975.

152 - VERCHEVAL, J., Un effet géomagnétique dans la thermosphère moyenne, 1975.

153 - AMAYENC, P., D. ALCAYDE and G. KOCKARTS, Solar extreme ultraviolet heating and dynamical processes in the mid-latitude thermosphere, 1975.

154 - ARIJS, E. and D. NEVEJANS, A programmable control unit for a balloon borne quadrupole mass spectrometer, 1975.

155 - VERCHEVAL, J., Variations of exospheric temperature and atmospheric composition between 150 and 1100 km in relation to the semi-annual effect, 1975.

156 - NICOLET, M., Stratospheric Ozone : An introduction to its study, 1975.

157 - WEILL, G., J. CHRISTOPHE, C. LIPPENS, M. ACKERMAN and Y. SAHAI, Stratospheric balloon observations of the southern intertropical arc of airglow in the southern american aera, 1976.

158 - ACKERMAN, M., D. FRIMOUT, M. GOTTIGNIES, C. MULLER, Stratospheric HCl from infrared spectra, 1976.

159 - NICOLET, M., Conscience scientifique face à l'environnement atmosphérique, 1976.

160 - KOCKARTS, G., Absorption and photodissociation in the Schumann-Runge bands of molecular oxygen in the terrestrial atmosphere, 1976.

161 - LEMAIRE, J., Steady state plasmapause positions deduced from McIlwain's electric field models, 1976.

162 - ROTH, M., The plasmapause as a plasma sheath : A minimum thickness, 1976.

163 - FRIMOUT, D., C. LIPPENS, P.C. SIMON, E. VAN HEMELRIJCK, E. VAN RANSBEECK et A. REHRI, Lâchers de monoxyde d'azote entre 80 et 105 km d'altitude. Description des charges utiles et des moyens d'observation, 1976.

164 - LEMAIRE, J. and L.F. BURLAGA, Diamagnetic boundary layers : a kinetic theory, 1976.

165 - TURNER, J.M., L.F. BURLAGA, N.F. NESS and J. LEMAIRE, Magnetic holes in the solar wind, 1976.

166 - LEMAIRE, J. and M. ROTH, Penetration of solar wind plasma elements into the magnetosphere, 1976.

167 - VAN HEMELRIJCK, E. et H. DEBEHOGNE, Réduction de clichés de champs stellaires pris par télévision avec intensificateur d'image, 1976.

168 - BRASSEUR, G. and J. LEMAIRE, Fitting of hydrodynamic and kinetic solar wind models, 1976.